

Simulating glacier mass balance in the cross-border Poiqu/Bhotekoshi Basin, China and Nepal

Bo Kong, Huan Yu, Wei Deng and Qing Wang

ABSTRACT

To assess the change of glacier mass balance (GMB) in the Poiqu/Bhotekoshi basin in the context of global warming, this study applied a conceptual Hydrologiska Bryans Vattenbalansavdelning (HBV) hydrological model to quantify the GMB in the area. The HBV model was trained and validated based on in-situ hydro meteorological data from 10 weather stations in the basin. The dataset, which consists of the daily observations for both rainfall and air temperature, was partitioned into two decades, 1988–1998 and 1999–2008 for calibration and validation, respectively. The calibrated model was adopted to restore the daily runoff depth and then estimate the annual changes of GMB in Poiqu/Bhotekoshi basin over the period of 1988–2008. Results show that the Nash–Sutcliffe efficiency coefficient (R_{eff}) of the daily runoff depth simulation after the runoff calibration process was above 0.802. Therefore, the simulated values of the HBV model are reliable and can be used to estimate the GMB of Himalayan cross-border glacial mountain basins with huge elevation difference, and provide scientific data support for water resources management. Furthermore, the result demonstrated a slow year-by-year rise of snow water equivalent because of global warming, and it highly correlates with the soil moisture, the spring temperature and the summer precipitation.

Key words | conceptual hydrological model, cross-border rivers, glacier mass balance, Poiqu/Bhotekoshi Basin, runoff depth

Bo Kong

Wei Deng

Institute of Mountain Hazards and Environment,
Chinese Academy of Sciences,
Chengdu, 610041,
China

Huan Yu (corresponding author)

College of Earth Sciences,
Chengdu University of Technology,
Chengdu, 610041,
China
E-mail: yuhuan0622@126.com

Qing Wang

Department of Geography and Environmental
Resources,
Southern Illinois University,
Carbondale, 62901,
USA

HIGHLIGHTS

- The HBV model had a better simulation effect on the annual daily runoff depth.
- The HBV model parameter combination was obtained through calibration.
- The precipitation increase was found to have a contribution rate of 38% to runoff.
- Glacial melting caused by temperature had a contribution rate of 62% to runoff increase.

INTRODUCTION

In many mid-latitude mountain regions, glaciers act as a temporal water storage such that new snow falls to nourish the glaciers in winter and then melts in summer (Jansson *et al.* 2003). Normally, the glaciers in these regions can keep a balance between the melting and nourishing, however such balance is at risk due to the climate change. Recently, glacier

shrinkage has become increasingly serious and has drawn much attention from the public. The most crucial concern is that the shrinking glaciers are likely to cause water loss and stream-flow variability, particularly during the dry seasons of the year (Braun *et al.* 2000; Collins 2008; Moore *et al.* 2009). At transnational level, the concerns regarding the mid-latitude glacier shrinkage mainly concentrate on the accessibility of water resources, which has caused disputes and even conflicts among countries. Poiqu/Bhotekoshi basin, a mid-latitude transnational region between China and Nepal, is currently

This is an Open Access article distributed under the terms of the Creative Commons Attribution Licence (CC BY 4.0), which permits copying, adaptation and redistribution, provided the original work is properly cited (<http://creativecommons.org/licenses/by/4.0/>).

doi: 10.2166/wcc.2020.024

confronting the imbalance between glacier recharging and discharging (Fujita & Ageta 2000). A quantitative assessment of the glacier loss is urgently needed in order to support environmental decision making.

In this study, a hydrological conceptual framework is considered to support the quantification of the glacier loss. The conceptual model used by this study is different from the physical model. The physical model is based on the hydrological process research using experimental methods. However, some measured data of cross-border basins are very difficult to obtain. The conceptual model generalizes the physical basis of the basin, and then combines the hydrological empirical formula to approximate the flow process of the basin. The basic idea is to model the runoff during the melting season as compared to the rainfall or snow nourishment such that the GMB can be estimated. The main challenges of this study come from several aspects. First, the existing hydrologic models that are mostly developed for estimating the contribution of melted ice sourced from the mountain snow peak, which could not provide a straightforward inference for estimating the runoff caused by mid-latitude glacial melting. It is worth noting that many scholars have made great progress in the study of glacial runoff at very high altitudes in recent years (Zhu *et al.* 2016; Yin *et al.* 2017), especially in the estimation of runoff using the improved HBV model at a glacierized alpine catchment (Wang *et al.* 2019). Second, the runoff in high elevation upstream basins can be contributed by either ice or snow, and therefore an analytical separation is required to identify the flows from the melting glaciers. In addition, the bad transportation conditions in the study area led to the rarity of in-situ hydrological data. Despite the dataset being adequate in the context of temporal information, only 12 weather stations were sparsely distributed over the basin. To resolve the abovementioned concerns, a runoff model that provides separate estimations for ice and snow and is capable of handling 'small' datasets is significantly necessary (Kulkarni *et al.* 2002; Zhao *et al.* 2013; Sun *et al.* 2015).

A large number of previous studies have shown that the methodological development in glacial hydrology has gone through three stages, namely empirical statistical modeling, analytical modeling, and numerical modeling (Chen *et al.* 2003). The first two stages appeared in the 1970s and have no obvious temporal order in the application to estimate glacier runoff. Since the early 1990s, simple statistical models

started fading in the applications of simulating glacier runoff. On the other hand, the conceptual glacier hydrological model was in development on the basis of formulating the physical process of the glacier runoff. Until the late 1990s, Arnold *et al.* (1998) applied the numerical modeling technique 'distributed hydrological modeling' to study the glacier hydrology. Distributed hydrological modeling could truly describe and scientifically reveal the natural spatio-temporal dynamics in the context of the hydrological circle, and opened a new era of glacier hydrological modeling (Arnold *et al.* 1998).

Since the HBV model was successfully applied to predicting the possible change of the runoff in an inland mountainous river basin under the conditions of climate change, many variations of HBV have been developed (Bergström 1976; Kang *et al.* 1999; McIntyre *et al.* 2013). The advantages of using HBV-based models mainly come from the fact that they can estimate the runoff from both snow and ice melting, and are also highly tolerant to a small number of training samples. Moreover, HBVs are capable of modeling the glacier runoff across different river basin regions (Bergström 1992; Jost *et al.* 2012). The studies of HBV have focused on the topics of sensitivity and uncertainty analysis targeted at the model parameters since the 1990s (Abebe *et al.* 2010; Chen *et al.* 2012; Li & Xu 2014; Nourali *et al.* 2016), the contrastive study between the HBV model and other hydrological models (Clark & Kavetski 2010; Kavetski & Clark 2010), the model application under different climate conditions (Braun & Renner 1992; Liden & Harlin 2000; Li *et al.* 2013), and integrating the HBV model with climate models through which the influence of climate change on the runoff can be investigated (Menzeil & Burger 2002; Gardelin *et al.* 2003; Hagg *et al.* 2007).

As one variation of the conceptual HBV model, the glacier melt runoff was rescaled by elevations in order to be adapted to simulate the Heihe mountain runoff in the north of China (Kang *et al.* 1999, 2002). Despite Kang *et al.* (1999, 2002) computing the runoff contributions from ice/snow and rain separately, their description of the runoff formation process was incomplete, for instance, the infiltration and melt water refreezing were not considered. This study added infiltration and melt water refreezing factors to the model, and a complete conceptual HBV model was proposed and then applied in the Poiqu/Bhotekoshi basin to simulate the runoff process and assess the changes of GMB.

The objectives of this paper are: (a) to establish a conceptual hydrology model that simulates the glacier melt runoff in the cross-border region between the Poiqu basin, China, and Bhotekoshi basin, Nepal; (b) to estimate the sensitivity of simulation factors for this model in a glacier-fed zone transitioning from a higher altitude to a lower altitude; and (c) to assess the change of GMB in Poiqu/Bhotekoshi basin and support the environmental decision making.

SITE DESCRIPTION AND DATA

Study area

Poiqu/Bhotekoshi, a tributary of the Cauchy River in the Ganges upstream, is one of the main water resources of Nepal, and since it flows across three countries, it is an important and invaluable topic in transnational environmental management (Figure 1). Poiqu/Bhotekoshi river,



Figure 1 | Position of the Poiqu/Bhotekoshi basin within Nepal and China.

which originates in Nyalam County, China ($85^{\circ}25' - E86^{\circ}30'E$, $27^{\circ}30' - N28^{\circ}35'N$), is 117 km long covering an area of 2,018.41 km². In this river basin, the altitude changes rapidly from 4,554 to 616 m, which leads to a convergence of various climate, soil types, and landscapes. The precipitation in Poiqu/Bhotekoshi basin is spatially imbalanced; the northern Himalayas have 300–400 mm yearly rainfall, while the annual precipitation usually stays between 1,000 and 1,500 mm in the south (subtropical and tropical area). The annual rainfall in the middle Poiqu/Bhotekoshi basin can also reach more than 1,000 mm, however a large amount of annual evaporation is observed. The ecological degradation, population concentration and the unbalanced distribution of precipitation, which in turn lead to serious soil erosion, attribute a dry characteristic to the valley area. The basins are widely spread from the most southern region to Zhangmu-Nyalamu region (above 5,000 m), and the corresponding surface soil content changes from southern alluvial soil and mountain red soil to the yellow brown soil and cold desert soil. From south to north, the vegetation type changes from coniferous/broad-leaved to shrub/meadow. In this study area, the relative elevation difference is large, so the simple statistical model is not suitable for glacier runoff simulation. The introduction of conceptual glacier hydrological model HBV focuses on the physical process of glacier runoff formation, which is helpful for the accuracy of simulating runoff and material balance.

Data

Due to the complexity of the conceptual HBV model, various factors (model input) are required, including daily average temperature, daily precipitation, monthly potential evaporation, temperature gradient, and annual precipitation gradient. In this study, the daily precipitation, daily temperature and monthly evaporation data were collected from 10 weather stations during the period 1988–2008. Among these stations, the upstream stations include Nielamu, Gumthang, Sundarijal and Zhibin, the midstream stations include Jiri, Dolalghat and Busti, and the downstream stations include Pandhera, Dobhan and Panchkhal. Runoff observations were acquired from three hydrometric stations from 1988 to 2008 (Figure 1). The meteorological data units involved in the model are different, but the standard unit

values of snow water equivalent, evapotranspiration, soil storage and runoff are finally obtained through the calculation of nonlinear equations. To fill the dates with no meteorological observations, a combination of the precipitation gradient technique and multivariate regression was applied to reproduce the data. If there are missing daily rainfall data between 1988 and 2008, these two algorithms can fill the gap of missing daily rainfall data. The land use/land cover (LULC) map was obtained by using object-oriented classification based on the Anderson classification system (Anderson 1976). The accuracy of classification results is 84.5% compared with field validation. This data was used in the model setting, that is, land use data was used to calculate land use area at different altitudes in different ecosystems. As observed from the weather stations, the temperature drops at a rate of $-0.61^{\circ}C/1,000$ m as the elevation increases. However, precipitation has a positive relationship to the elevation: an average 25 mm precipitation increase corresponds to every 1,000 m elevation rise.

METHODS

An HBV technique, considered as a semi-distributed conceptual basin hydrological model, was developed by the Swedish Meteorological and Hydrological Research Institute based on the characteristics of the basins in the Nordic region (Bergström 1976). Its advantage lies in the parameterization of the physical processes of runoff generation and confluence based on the principle of water and energy balance, which has a clear physical concept. HBV is a semi-distributed model in which the catchments could be separated into three elevations and seven vegetation zones. By using daily precipitation and air temperature data, such a model may be used to simulate the basin daily runoff (Figure 2) (Seibert & Vis 2012). The daily meteorological hydrological data from 1988 to 2008 were divided into two groups (the standard value of 1988–1998, and the reference value of 1999–2008). By using the Thiessen polygon method, the spatio-temporal interpolation of continuous daily precipitation value was conducted based on the precipitation data of six stations (Nyalum, Gumthang, Barhabise, Dhaph, Nawalpur and Chautara). Then, the temperature data in two of the stations (Nyalum and Panchkhal) were used to estimate the daily average temperatures of the Poiqu/Bhotekoshi basin.

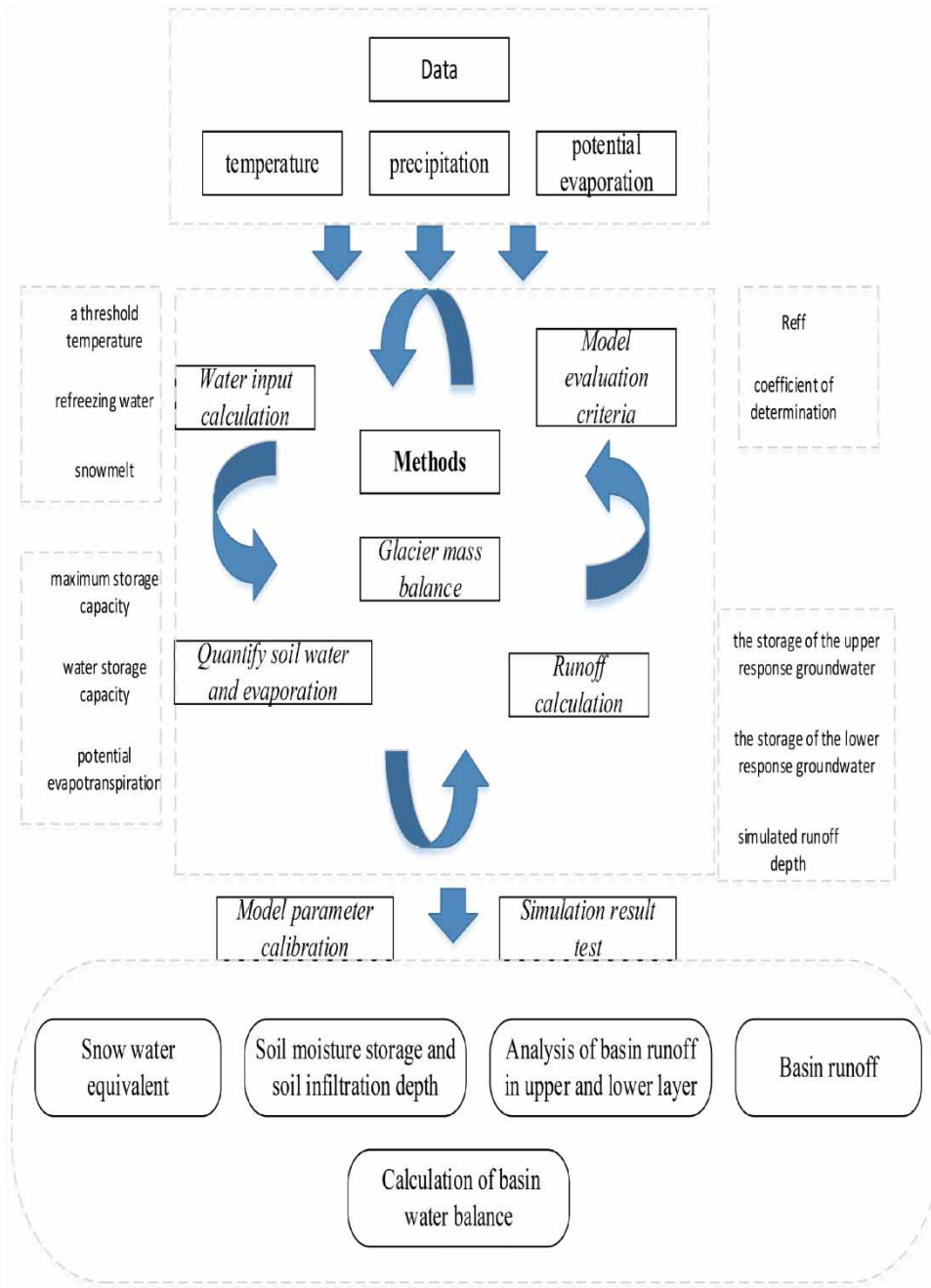


Figure 2 | A process chart illustrating the structure and relationships of all models.

Water input calculation

In the study area, glacier melting, snow melting and rainfall are the main sources of basin runoff. Note that rainfall was

considered as snowfall if the air temperature was below a threshold temperature T_0 ($^{\circ}\text{C}$). After the accumulated snow on top of the glacier has melted completely, the amount of glacier melting is termed as an ice melting volume (Equations (1)

Table 1 | Description of method parameters

Parameter	Parameter significance
F	Volume of refreezing water
C _f	Refreezing coefficient
T	Average temperature
T ₀	Threshold temperature
M	Volume of snowmelt
C _m	Coefficient of snow melting
M _i	Ice melting volume
R	Coefficient of calibration so that the effect of elevation on ice melting is normalized. Different altitudes can affect the calculation of ice melting. The r is used to prevent the influence of calculation errors caused by this altitude
SM	Maximum storage capacity of soil layer at different altitudes
FC	Water storage capacity of soil layer
B	Water storage coefficient
L _p	Demand volume of soil water under the condition of limited evaporation. L _p controls soil evapotranspiration
E _p	Actual evapotranspiration
E	Potential evapotranspiration
K ₁	Outflow coefficient of the soil flow in the upper response groundwater
SUG	Storage of the upper response groundwater
K ₂	Outflow coefficient of soil flow in the lower response groundwater
SLG	Storage of the lower response groundwater
K ₀	Determined by whether the SUG upper response area is greater than the threshold UGL
T	Observation period, and here it demotes the day
i	A counter, which is an important variable in the sum equation
u	An important parameter in the triangular weight equation
P_MAXBAS	A shape parameter, which is related to basin area. The larger the area, the bigger the P_MAXBAS value, and the faster corresponding confluence process
Q _{obs}	Observed runoff depth
$\overline{Q_{obs}}$	Observed mean value
Q _{sim}	Simulated runoff depth
$\overline{Q_{sim}}$	Simulated mean value
B	Glacier mass balance (GMB)
P	Precipitation
E _g	Basin surface evaporation

and (2)) (Table 1) (Hottelet *et al.* 1993; Konz & Seibert 2010):

$$\begin{cases} F = C_f(T_0 - T) & T \leq T_0 \\ M = C_m(T - T_0) & T \geq T_0 \end{cases} \quad (1)$$

$$M_i = rC_m(T - T_0) \quad (2)$$

Quantify soil water and evaporation

According to the concept of HBV, the soil moisture layer (SML) is defined as the layer that is below the soil surface and above the depth of active permafrost or water table. In Equation (3), WR (mm) is the amount of seepage water that travels to the glacier and SML from different sources, and RO is the soil infiltration depth that calculates the water flux from soil to groundwater aquifer (Seibert & Vis 2012). Their relationships are given as (Table 1):

$$RO = \begin{cases} WR(SM/FC)^\beta & SM < FC \\ WR, & SM \geq FC \end{cases} \quad (3)$$

A soil-box experimental model of evaporation, E_p , is given as:

$$E_p = \begin{cases} E(SM/L_p), & SM < L_p \\ E_p, & SM \geq L_p \end{cases} \quad (4)$$

when SM is less than L_p , the ratio of actual evapotranspiration (E_p) to potential evapotranspiration (E) is linear with soil moisture; when the SM is greater than L_p , E_p is equal to E .

Runoff calculation

Two runoff parameters – runoff in response to groundwater (Q_{GW}) and simulated runoff depth (Q_{sim}) – are calculated as (Table 1) (Bergström & Singh 1995):

$$Q_{GW}(t) = K_2 \cdot SLG + K_1 \cdot SUG + K_0 \cdot \max(SUG - UGL, 0) \quad (5)$$

$$Q_{sim}(t) = \sum_{i=1}^{P_{MAXBAS}} c(i) \cdot Q_{gw}(t - i + 1) \quad (6)$$

where:

$$c(i) = \int_{i-1} \frac{2}{P_{MAXBAS}} - \left| u - \frac{P_{MAXBAS}}{2} \right| \cdot \frac{4}{P_{MAXBAS}^2} du \quad (7)$$

Equations (5)–(7) were proposed as a variation of the traditional conceptual HBV model. Our modifications mainly take into account the seasonal and annual variation characteristics of the glacier system. Newly developed equilibrium line altitudes were deduced from our observations and then employed to standardize the model calibration process for the regions with different elevations, such as accumulation zone and melting zone. The determination of the glacier equilibrium line height is very important for the calculation of the HBV model, because it can eliminate the calibration fuzziness of model parameters SFCF, CFR and FC (Table 1).

Model evaluation criteria

The R_{eff} and coefficient of determination (r^2) (Equations (8) and (9)) were employed in this study to test the model accuracy (Nash & Sutcliffe 1970; Seibert 2005). While interpreting both indices, 1 indicates perfect performance and 0 is poor (Table 1).

$$R_{eff} = 1 - \frac{\sum (Q_{obs} - Q_{sim})^2}{\sum (Q_{obs} - \overline{Q_{obs}})^2} \quad (8)$$

$$r^2 = \frac{[\sum (Q_{obs} - \overline{Q_{obs}})(Q_{sim} - \overline{Q_{sim}})]^2}{\sum (Q_{obs} - \overline{Q_{obs}})^2 \sum (Q_{sim} - \overline{Q_{sim}})^2} \quad (9)$$

Table 2 | Land use type area of Poiqu/Bhotekoshi basin at different altitudes (km²)

Division level		Glacier ecosystem V2			Forest ecosystem V1			
		Glacier	Bare rock soil	Grassland	Woodland	Cropland	Water area	Settlement
Total area		214.98	9.55	14.11	353.77	144.74	3.37	0.50
Altitude	< 1,800	0.00	0.01	0.00	68.05	99.68	2.62	0.31
	1,800–3,000	0.64	0.14	0.55	171.07	45.04	0.69	0.19
	3,000–5,000	214.34	9.40	13.56	114.65	0.02	0.06	0.00

Glacier mass balance

In accordance with the basin precipitation, runoff, and soil evaporation data were obtained by the model (Equation (10)), and are based on the principle of the water balance (Table 1):

$$B = P - Q_{sim} - E_p - E_g \quad (10)$$

Model settings

The daily observations were partitioned into three different time intervals: 7, 14, and 30 days. These three values are the set values of the model, reflecting the changes of runoff in 1 week, 2 weeks and one month. In accordance with the runoff observations in the study area, we defined the runoff volume, Q_{obs} , as follows: less than 0.1 as extreme dry year; 0.1–0.5 as dry year; 0.5–1 as normal year; 1–2 as wet year; and $Q_{obs} > 2$ as extreme wet year. These five thresholds are obtained by repeated calculation of the model, reflecting the real five grade indexes of the runoff anomaly change of Poiqu/Bhotekoshi Basin. Based on the above definition, the annual runoff data were classified into different categories. To prevent duplication, the data from closely adjacent stations were aggregated and allocated to the lower reaches of the basin. To avoid the high computational cost, the altitude was discretized into three levels: <1,800, 1,800–3,000, and 3,000–5,000 m. The land cover types were organized into two major ecosystems – glacier and forest (Table 2).

MODEL SIMULATION AND TEST

Model parameter calibration

To calibrate the model parameters, we combined a genetic algorithm (GA) with a trial and error method, along with

visual examination. The R_{eff} was used for the simulation of the standard value, and the reference value was used for the parameter setting. High quality data (1988–1998) was used for the parameter calibration in order to obtain a comprehensive model parameter (Table 2). The sensitivity of the model was tested for 15 parameters (Table 3), and it was found to be significantly sensitive to recession coefficient K_1 , the snow adjustment factor and the soil field water-holding capacity, and also relatively sensitive to threshold temperature (TT), refreezing meltwater (CFR), a certain portion of the water equivalent of the snow pack (CWH), lower base flow recession coefficient (K_2) and max percolation to lower zone (PERC). In order to test the model efficiency, the calibrated parameters were used to conduct the non-parameter calibration. In this study, the data from 1999 to 2008 were adopted to validate the model test. The value of the first 10 years is used to calibrate the simulation model, and the second 10 years is used to verify the accuracy of the future prediction. The accuracy of calculation results is relatively high, which denotes that the model is feasible. The R_{eff} of the observed value and simulated value were 0.84 and 0.80, respectively (Figure 3).

Simulation result test

After the model simulation, the simulation results and the efficiency coefficient of each year were obtained. The best R^2 was 0.84 and the worst year reached 0.80, indicating that the model could explain more than 80% of the flow generation process in the basin (Figure 3). In terms of simulation accuracy, our model was successful in the study area. This benefits from the setting that the model takes into account both the glacier melting runoff in summer and snow water equivalent in winter, which results in the simulated values being close to the actual observed value. However, the degree-day factor method of the glacier melting simulation in the model had insurmountable defects. For example, with the increase of the time resolution, the simulation precision lowered (Hock 2003). Therefore, when comparing the model simulation with the observed monthly runoff depth (Table 4 and Figure 4), the effect was higher than the precision of the daily runoff depth. In addition, the correlation R^2 between the simulated monthly runoff depth and the observed value was as high as 0.98. In contrast with the annual runoff depth, the error in the

Table 3 | Model parameters of Poiqu/Bhotekoshi basin

Layer level	Parameter significance	Parameter	Parameter relevance	Parameter range	Parameter value
Glacier module	Threshold temperature ($^{\circ}\text{C}$)	TT	+	-1-2.7	2.49
	Max. meltwater parameter in a degree-day method ($\text{mm d}^{-1}\text{ }^{\circ}\text{C}^{-1}$)	CFMAX	+	0 ~ 1	0.5
	Correction factor ($\text{mm d}^{-1}\text{ }^{\circ}\text{C}^{-1}$)	SFCF	+++	0.4-1	0.99
	Refreezing meltwater ($\text{mm d}^{-1}\text{ }^{\circ}\text{C}^{-1}$)	CFR	+	0-1	0.09
	A certain portion of the water equivalent of the snow pack ($\text{mm d}^{-1}\text{ }^{\circ}\text{C}^{-1}$)	CWH	+	0-1	0.1
Soil moisture layer	A model parameter values of field capacity (mm)	FC	+++	50-500	220
	Soil moisture value above which actual evaporation reaches potential (mm)	LP	-	0.3-1	0.99
	Parameter that determines the relative contribution to runoff from rain or snowmelt (-)	BETA	+	1-6	1
Underground water and response module	Max. percolation to lower zone	PERC	++	0-6	6.7
	Max. storage in zone, threshold parameter (mm)	UZL		10-50	30
	Flood peak recession coefficient (d^{-1})	K0	+++	0-1	0.25
	Upper interflow recession coefficient (d^{-1})	K1	+++	0.01-0.2	0.04
	Lower base flow recession coefficient (d^{-1})	K2	++	0.001-0.2	0.14
	One free parameter in a equilateral triangular weighting function	MAXBAS	-	1-7	1.28
Evapotranspiration	Temperature related factor ($^{\circ}\text{C}^{-1}$)	Cet	-	1-10	3.03

Notes: + denotes the strength of parameter correlation; - denotes no relevance.

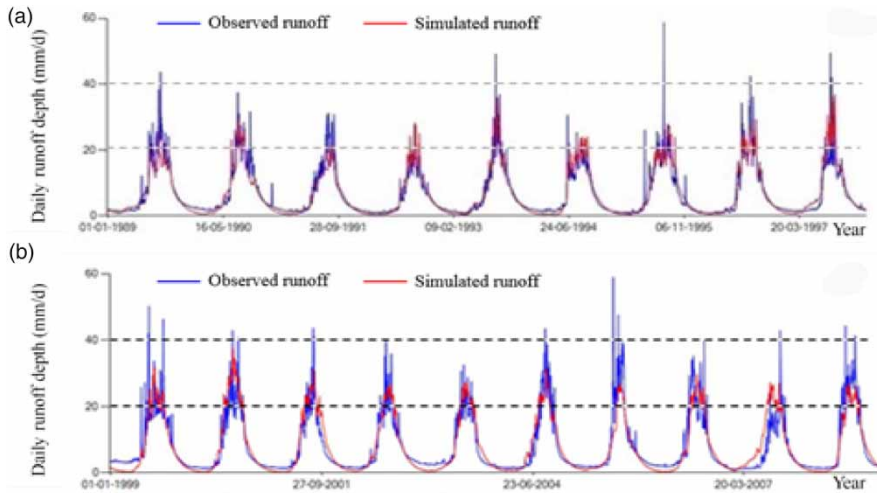


Figure 3 | Simulated and observed daily runoff depth from 1988 to 2008: (a) calibration period: 1988–1998; and (b) validation period: 1999–2008.

maximum annual runoff depth was less than 6% during the model validation (Table 4). Since there is no practical significance for analyzing other months because of the dry season with less runoff, the precision was considered to be acceptable. In summary, the model performs better in the simulation of monthly runoff depth than daily runoff depth, indicating that the changes in the monthly runoff depth obtained by the model were more acceptable.

RESULTS AND DISCUSSION

Besides the influence of precipitation and temperature, the Poiqu/Bhotekoshi basin may be associated with the terrain and water vapor sources crossing the Himalayas, where the summer precipitation is mainly affected by the Indian monsoon (Zhang et al. 1997). As we found in the results, the Poiqu/Bhotekoshi basin had a similar precipitation pattern to the Tamakosi basin, which ensured the accuracy of interpolation using the adjacent meteorological data. The daily precipitation, daily temperature, and daily runoff depth data in the last two decades were simulated and are shown in Figures 5 and 6, respectively.

The driving factor of the model

Rainfall and temperature are the two most important driving factors directly involved in daily operation in the HBV model, so we need to analyze both of them first.

Precipitation

In the past two decades, the daily rainfall in the Poiqu/Bhotekoshi basin changed roughly following the annual cycle. Only in a few months and a particular year was the daily precipitation found to be higher or lower. Some examples are as follows: the daily precipitation in July 2008 reached 140 mm; the whole-year precipitation was higher in 1994 and 1995 (Figure 5); and June–August of every year was basically the abundant precipitation cycle. However, the trend observed from the station data was exhibited differently due to the variations in their altitude. In fact, the precipitation did not always decrease while the altitude got higher. The elevation range from 1,200 to 2,000 m had the precipitation gradually increase as the altitude increased. When the altitude reached a certain threshold, such as 4,000 m or greater, the precipitation was actually very low, and the multi-year average precipitation was only approximately 600 mm. The areas with relatively high precipitation were mainly concentrated on the southern Himalayas, which are primarily covered by coniferous and broad-leaved forest vegetation, and have less arid lands and paddy fields. During July–August, the precipitation was abundant, leading to frequent floods during the rainy season.

Temperature

Based on the in-situ meteorological observations, kriging interpolation was implemented to map the annual high,

Table 4 | Observed and simulated monthly runoff depths from June to October during 2001–2008

Runoff depths(mm)		2001		2002		2003		2004		2005		2006		2007		2008	
		O	S	O	S	O	S	O	S	O	S	O	S	O	S	O	S
6	863.9	835.1	1,012.0	930.1	653.4	609.5	597.7	588.8	200.5	182.2	484.3	458.8	642.1	780.1	1,470.6	1,373.0	
7	896.5	886.3	1,422.5	1,515.2	1,287.0	1,204.4	1,700.0	1,614.3	488.7	467.6	1,870.2	1,991.1	1,192.4	1,255.2	2,344.6	2,255.5	
8	1,780.0	1,567.7	1,439.6	1,560.5	1,462.1	1,403.1	1,295.1	1,240.6	1,770.6	1,709.7	1,997.4	2,188.8	811.2	854.5	1,840.5	1,793.3	
9	342.6	317.2	502.0	479.3	901.2	888.4	1,300.5	1,290.6	451.2	404.9	1,990.8	1,978.0	1,493.4	1,489.2	1,270.1	1,228.8	
10	200.5	173.1	81.3	80.7	168.2	165.5	480.6	432.1	490.1	487.1	65.4	62.6	33.1	46.4	65.2	42.6	
Total	4,083.5	3,779.4	4,457.4	4,565.8	4,471.9	4,270.9	5,373.9	5,166.4	3,401.1	3,251.5	6,408.1	6,679.3	2,772.2	4,425.4	6,991	6,693.2	

Notes: O, observed value; S, simulated value.

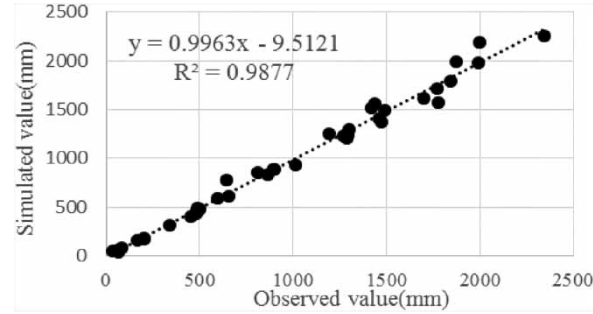


Figure 4 | Observed monthly runoff depth in comparison with that simulated from HBV model during 2001–2008.

annual average, and annual low temperature. After that, a comparison was made among these temperature estimations. The daily temperature changes also followed the annual cycle. The difference between the annual maximum and minimum temperature was 0.22–39.56 °C. However, the temperature increased with the altitude decline. At altitudes between 3,800 and 4,300 m, the annual average temperature was around 3.25–3.82 °C (Figure 6). However, a warming trend was shown on the northern Himalayas, where the temperature tendency rate was 0.32 °C × 10 a⁻¹. This may contribute to the accelerated snow melting in that region. When the altitude was approximately 2,000 m, the annual average temperature reached 14.56 °C. At altitudes between 1,300 and 1,400 m, the annual average temperature was 17–18.56 °C, which was higher than that at 2,000 m by 4 °C, and its maximum reached 36 °C. Furthermore, the temperature tendency rate was only 0.006 °C × 10 a⁻¹, and the elevation showed a slowly increasing trend. At the altitude of 900–1,000 m, the average annual temperature was 21.34 °C. At altitudes below 100 m near the equator, the temperature was very high, with the maximum temperature being as high as 39.56 °C, and the minimum temperature 2.35 °C.

The multiple regression method was adopted to obtain the daily average temperature of the Poiqu/Bhotekoshi basin based on the observation data of weather stations. At the same time, the daily precipitation data were also obtained. Through mathematical statistics, it was determined that in the last two decades the basin temperature and the precipitation showed upward trends with average changing rates of 0.15 °C × a⁻¹ and 0.97 mm × a⁻¹, respectively.

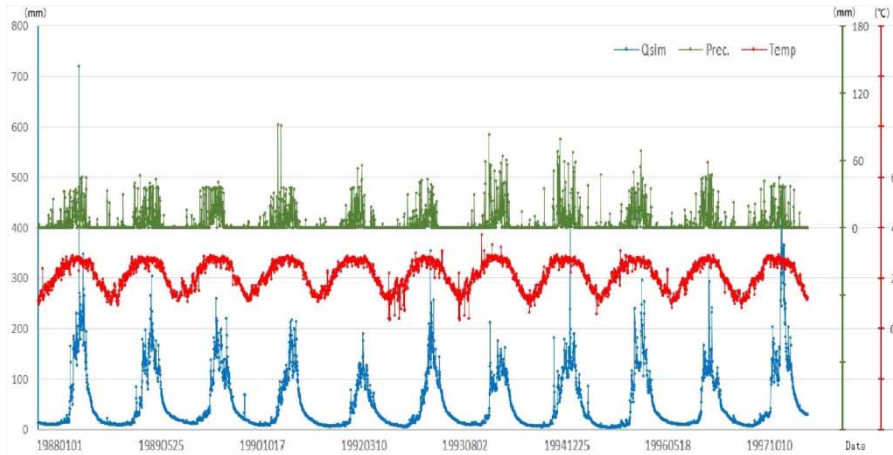


Figure 5 | Observed precipitation, air temperature, and simulated runoff depth from 1988 to 1998.

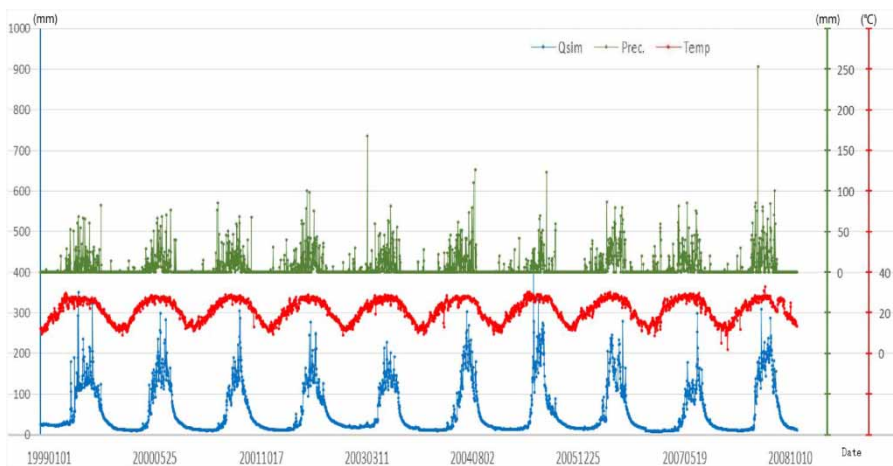


Figure 6 | Observed precipitation, air temperature, and simulated runoff depth from 1999 to 2008.

The simulated factor of the model

Snow water equivalent

Snow water equivalent in Poiqu/Bhotekoshi basin from 1988 to 2008 was calculated based on Equation (1) (Figure 7). The snow accumulation showed a significant decrease in the region with snow accumulating for less than 120 days during the 20-year period; the regions with increasing snow accumulation had snowy days of around 120–350 (Sun et al. 2014) and the area of stable snow cover was gradually expanding. According to the simulated snow water equivalent, the expanding regions of snow water

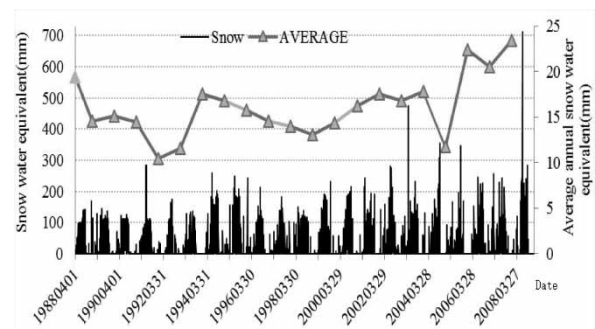


Figure 7 | Snow water equivalent of Poiqu/Bhotekoshi basin from 1988 to 2008 (AVERAGE denotes the average annual snow water equivalent, which refers to the average value of one year; Snow denotes the snow water equivalent, which refers to the value of 1 day).

equivalent were positively correlated with the snow accumulation days to a great extent. The snow water equivalent was increasing year by year while snow accumulation days were decreasing in Poiqu/Bhotekoshi basin (Figure 7), which may indicate a rising temperature causing a transition from perennial snow to seasonal snow while the snowfall was increased. The snow area was shrinking, while the maximal snow areas first showed a fluctuating increasing trend and a decreasing trend after that. The average accumulated snow showed a fluctuating decreasing trend with an annual rate of $-1.00 \times 10^3 \text{ m}^3 \times \text{a}^{-1}$. There was a gradual increase in snow water equivalent and the rise started at each fall. The drops of average annual snow water equivalent were 10.48 and 11.73 mm in 1992 and 2005 respectively, while the peaks were 17.59 and 22.38 mm in 1994 and 2006 respectively. From 2006 to 2008, snow water equivalent kept soaring, which was consistent with the previous finding of temperature rise and shrunken snow area. In summary, snow accumulation in most of the basin areas is decreasing year by year; on the other hand, the stable snow area is expanding and perennial snow cover is shrinking, which may be influenced by global warming.

Soil moisture storage and soil infiltration depth

Because the soil water content between the upper and lower layers is highly correlated, the soil water content in the upper layer can be estimated by using soil moisture storage in the lower layers through the HBV model. Soil moisture storage showed a nonlinear increasing trend in its depth (Figure 8), being consistent with the complexity of soil moisture of Poiqu/Bhotekoshi basin in a vertical direction.

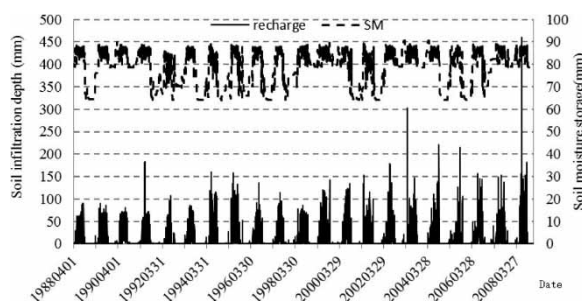


Figure 8 | Soil moisture storage and soil infiltration depth from 1988 to 2008 (recharge: Soil infiltration depth; SM: Soil moisture storage).

During the 20-year period, the soil moisture storage gradually increased with a daily rate of between 64.12 and 90.62 mm. The average values of winter–spring and summer–fall are 67 and 85 mm respectively, which demonstrates an obvious difference in water storage between dry and wet seasons (Figure 8). Many studies found that soil moisture storage was highly correlated with climate factors (Hou & Wulan 2006; Zhao et al. 2014). However, the correlation is also affected by the storage depth and observation season. The correlation coefficients between climate factors (temperature and precipitation) and soil moisture storage were calculated using SPSS software. We found that soil moisture storage was significantly affected by temperature as well as precipitation in the wet season. The results also illustrated that the rise of temperature drove permafrost and glacier to melt, which in turn increased the runoff.

The amount of soil water loss can be described by the soil infiltration depth in the HBV model. The soil infiltration depth showed a gradually increasing trend (Figure 8). Most of the high values, ranging from 80 to 150 mm, were observed in July or August with an infiltration rate of 0.08 mm/min. For particular months it reached more than 150 mm depth with an infiltration rate at 0.10 mm/min. The soil infiltration depth has a positive correlation with the soil moisture storage, in other words, both the snowmelt and rainfall have direct influences on the soil infiltration depth.

Simulation and analysis of basin water yield

Analysis of basin runoff in upper and lower layer

The basin runoff needs to be considered in two soil conditions, high permeability and low permeability. In the high permeability of the upper layer, the water level descends following the decreasing rainfall and soil infiltration without interception, then we define the storage threshold of the upper layer as UGL (Equation (5)). When the upper groundwater storage is greater than UGL, the runoff is determined by the coefficient K_0 . If it is less than UGL, the value will be determined by K_1 . In the low permeability of the lower layer, the groundwater level is no longer declining, or decreasing slowly, even if the rainfall and other factors are still dropping. The runoff in the lower layer is determined by the coefficient K_2 .

The storage in upper and lower groundwater and the runoff in upper/lower groundwater were simulated individually based on Equations (5)–(7). The simulation results are shown in Figures 9 and 10. The upper groundwater in Poiqu/Bhotekoshi basin is in an aquifer formed by metamorphic rocks, granites and shallow-water sedimentary rock of the Himalayas (Kazuo 1993). Because the aquifer has good water yield property, the regular or seasonal rainfall or snowfall are all likely to result in considerable storage volumes. The annual peak of the upper groundwater storage appeared in mid-August and varied between 140 and 200 mm (Figure 9). Within a year, the upper groundwater storage increased from March, reached the peak in August, and then fell back in early November. The lower layer is formed by metamorphism and weak metamorphic sedimentary rocks from Precambrian to Paleozoic.

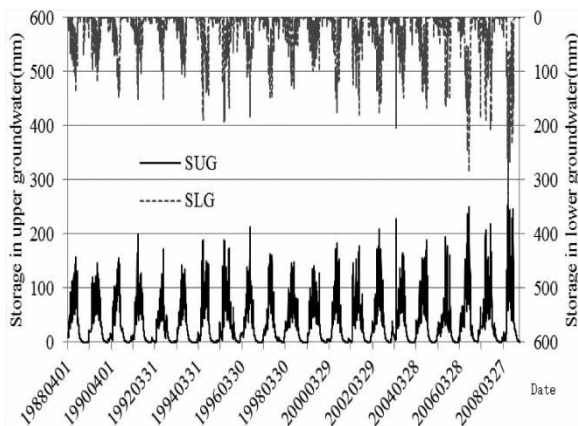


Figure 9 | Storage in upper and lower groundwater from 1988 to 2008 (SUG: Storage in upper groundwater; SLG: Storage in lower groundwater).

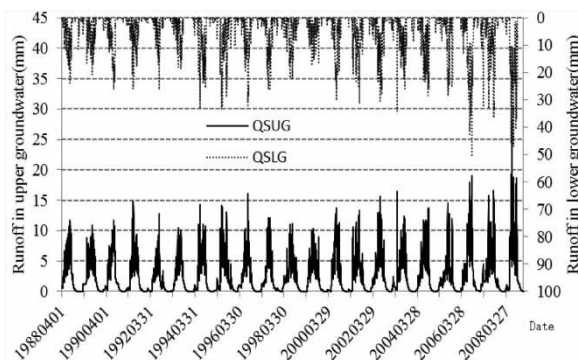


Figure 10 | Runoff in upper and lower groundwater from 1988 to 2008 (QSUG: Runoff in upper groundwater; QSLG: Runoff in lower groundwater).

Although the peak value of storage in the lower layer was also observed in August, the value only ranges from 120 to 180 mm. The seasons having an increasing water concentration were from July to early September, while the other months were lower than 50 mm. Compared to the upper level, the volume and recharging period in lower-level groundwater are significantly less or shorter than the upper level. As the lower layer has a larger elastic storage water rate, the contribution of periodic inland recharge on the storage is effectively reduced. In general, the contribution of the lower layer to groundwater storage is around 12–24% of the upper layer.

The total runoff in Poiqu/Bhotekoshi basin was calculated as the sum of the upper and the lower runoff (Figure 10). The water level of the upper groundwater goes up as the rainfall infiltration recharge increases. The correlation between the upper runoff, the storage and rainfall are quite significant. The simulation results show that the runoff in lower groundwater is twice as high as the upper level; on the other hand, the storage in lower groundwater is slightly lower than the upper level. When the surface water level rises, the underwater pressure increases, the water infiltration increases, and the peak value of groundwater runoff curve will be higher. In the season of heavy rainfall, the infiltration of rainwater also increases, and the peak value of groundwater runoff curve will be higher. One of the reasons is that the water level of the storage in upper groundwater is always greater than the lower, which leads the groundwater to flow downwards to the soil aquifer. Another reason is that part of the water flows into the sea due to the hydraulic gradient.

Basin runoff

In this study, the runoff was represented by the runoff depth. The daily runoff in the simulated annual cycle shows a similar overall trend. It increases in early January, peaks in August, and then declines in October. In August 1988, the maximum runoff reached 714 mm, and the maximum of other years ranged from 300 to 470 mm (Figure 4). According to the spatial pattern of the runoff depth in the Poiqu/Bhotekoshi basin, the runoff depth gradually increased from north to south. The runoff depth on the northern slope of the Himalayas was relatively lower

(0.97–340 mm), while the southern slope had an average of 200–2,100 mm. From May–September, the runoff depth increased until it peaked in August, and the overall monthly average was up to 574 mm with a minimum average of 327 mm. The periods with lower runoff depth were mainly in the dry season or winter, for example, January–April and October–December, as shown in Figure 5.

Calculation of basin water balance

The change of permafrost in the river basin contributes to less than 1% of the water balance (Zhang & Yao 2002). Therefore, it is reasonable to assume that the annual average soil moisture content in the study area did not change. In the calculation, the impact of the precipitation gradient was considered in the precipitation (P) (Equation (10)); E_p is the model simulation result; and E_g is the basin surface evaporation taken as the fixed value of 137.23 mm (Zhang & Yao 2002). When calculated with Equation (10), the basin mass balance from 1988 to 2008 had an average of $-135.85 \text{ mm} \times \text{a}^{-1}$. The simulated basin mass balance had a correlation coefficient of 0.77 ($\alpha = 0.01$) with the observed mass balance (Figure 11) (Pu et al. 1998; Fujita & Ageta 2000). We concluded that the model could effectively simulate each part of the water balance. The simulation results were reasonable, and the estimated model parameters could reflect a relatively true GMB in the Poiqu/Bhotekoshi basin.

Bhanu et al. (2016) conducted a simple hydrological calculation using the annual calculation and absorption from snow meteorological and discharge data, and analyzed the GMB observation values of Indian Himalaya over the last 40 years. Their results are close to the simulated values in our study, and the general trend is consistent with ours.

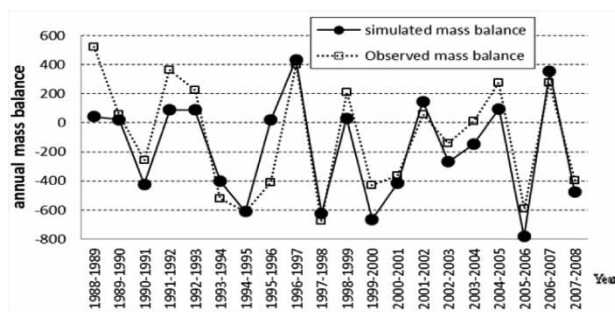


Figure 11 | Observed and simulated annual mass balance of the Poiqu/Bhotekoshi basin.

Etienne et al. (2007) used remote sensing technology to estimate GMB. Although the low value range of GMB estimated by the author is between -850 and $-700 \text{ mm} \times \text{a}^{-1}$, which is lower than the estimated value in our study, the glacier loss rate between 1999 and 2008 is twice that of 1988–1998, which is consistent with the analysis trend in our study. Ann et al. (2015) analyzed the response of GMB to climate change. Their model ignored the physical causality between input and output, which was not conducive to the analysis of the intermediate hydrological process, and our model overcomes this shortcoming.

CONCLUSIONS

The calibrated HBV was implemented in the transnational Poiqu/Bhotekoshi basin. The model first simulated the forming and flowing process of the runoff in the river basin, where the LULC could be classified as alpine tundra zone and a mountain vegetation zone. The glacier area accounts for 29% of the total area of the basin, and the effect of glacier ablation on the basin is very important. Therefore, the accuracy of the model for the glacier ablation simulation greatly affects the accuracy of the model for runoff simulation. The main advantage of the HBV model method is that it needs less data. The value of 1988–1998 was used to calibrate the model, and the value of 1999–2008 was used to verify the accuracy of future prediction. R^2 was 0.84, indicating that the model is feasible. Then, the model performs using some initial inputs, which were the in-situ monthly observations of temperature and precipitation, to simulate the traffic trails as well as to forecast the possible changes of the runoff in response to the climate change. This model can now be used to perform some monthly mountainous traffic trail forecasting based on the Poiqu/Bhotekoshi basin, which is located in a particular zone transitioning from a higher altitude to a lower altitude.

From the analysis of glacier/snow modules, soil modules and groundwater module, the days of snow accumulation in the Himalayas was decreasing, in particular, the permanent snow area is shrinking with an annual rate of $-1.00 \times 10^3 \text{ m}^3 \text{ a}^{-1}$ because of global warming. The stable snow area was increasing, which results in a slow rise of snow water equivalent. The annual soil moisture storage was mainly

affected by air temperature, and the correlations between soil moisture and temperature in spring, and soil moisture and rainfall in summer were the most significant. The model also simulated the storage and runoff of the most important groundwater response area. The simulation was performed on two soil layers, and then the water mass balance values were calculated. The R_{eff} of the daily runoff depth simulation after the runoff calibration process was above 0.80. Therefore, the HBV model had a good simulation efficiency on the annual daily runoff depth in the Himalayan cross-river glacial mountains. The water and heat conditions of glaciers in the Himalayas are constantly fluctuating, and the annual material balance is also different. Sometimes the accumulated amount is greater than the melting amount, and a positive balance appears, which is conducive to the development of Himalayan glaciers; otherwise, it will produce negative balance, leading to glacier shrinking.

The results show that the simulated values of the HBV model are reliable and can be used to estimate the GMB of cross-border mountain basins with huge elevation difference, and provide scientific data support for water resources management. However, in this study, hydrological observation data and evapotranspiration data were inadequate, and more abundant model-driven data can further improve the simulation accuracy. In addition, hydrological and underlying surface data can be used to regionalize the parameters and provide scientific data support for hydrological forecasting in the future study.

ACKNOWLEDGEMENTS

This study was supported by the National Natural Science Funds of China (grant no. 41971226; 41871357), the ‘One-Three-Five’ Project of Chinese Academy of Sciences (grant no. SDS-135-1708) and the Strategic Priority Research Program of the Chinese Academy of Sciences (XDA19030303).

DATA AVAILABILITY STATEMENT

All relevant data are included in the paper or its Supplementary Information.

REFERENCES

- Abebe, N. A., Ogden, F. L. & Pradhan, N. R. 2010 Sensitivity and uncertainty analysis of the conceptual HBV rainfall–runoff model: implications for parameter estimation. *J. Hydrol.* **389** (3–4), 301–310.
- Anderson, J. R. 1976 *A Land use and Land Cover Classification System for use with Remote Sensor Data*. Geological Survey Professional Paper No. 964 U.S. Government Printing Office, Washington, DC, p. 28.
- Ann, V. R., David, L. E., Duncan, J. Q. & Neil, F. G. 2015 Modelling the feedbacks between mass balance, ice flow and debris transport to predict the response to climate change of debris-covered glaciers in the Himalaya. *Earth Planet. Sci. Lett.* **430**, 427–438.
- Arnold, N., Richards, K., Willis, I. & Sharp, M. 1998 Initial results from a distributed, physically based model of glacier hydrology. *Hydrol. Processes* **12** (2), 191–219.
- Bergström, S. 1976 *Development and Application of A Conceptual Runoff Model for Scandinavian Catchments*. SMHI Report RHO No.7, Norrköping, Sweden.
- Bergström, S. 1992 *The HBV Model – Its Structure and Applications*. SMHI Report RH No.4, Norrköping, Sweden.
- Bergström, S. & Singh, V. 1995 The HBV model. In: *Computer Models of Watershed Hydrology* (V. P. Singh, ed.). Water Resources Publications, Highlands Ranch, CO, USA, pp. 443–476.
- Bhanu, P., Dwarika, P. D., Rakesh, B., Manish, M. & Vinod, C. T. 2016 Four decades of glacier mass balance observations in the Indian Himalaya. *Reg. Environ. Change* **16**, 643–658.
- Braun, L. N. & Renner, C. B. 1992 Application of a conceptual runoff model in different physiographic regions of Switzerland. *Hydrol. Sci.* **37** (3), 217–231.
- Braun, L. N., Weber, M. & Schulz, M. 2000 Consequences of climate change for runoff from Alpine regions. *Ann. Glaciol.* **31**, 19–25.
- Chen, R. S., Kang, E. S., Yang, J. P. & Zhang, J. S. 2003 A distributed runoff model for inland mountainous river basin of Northwest China. *J. Geog. Sci.* **13** (3), 363–372.
- Chen, H., Xu, C. Y. & Guo, S. L. 2012 Comparison and evaluation of multiple GCMs, statistical downscaling and hydrological models in the study of climate change impacts on runoff. *J. Hydrol.* **434**, 36–45.
- Clark, M. P. & Kavetski, D. 2010 Ancient numerical daemons of conceptual hydrological modeling: 1. Fidelity and efficiency of time stepping schemes. *Water Resour. Res.* **46** (10), 1–23.
- Collins, D. N. 2008 Climatic warming, glacier recession and runoff from Alpine basins after the Little Ice Age maximum. *Ann. Glaciol.* **48**, 119–124.
- Etienne, B., Yves, A., Rajesh, K., Sarfaraz, A., Patrick, W. & Pierre, C. 2007 Remote sensing estimates of glacier mass balances in the Himachal Pradesh (Western Himalaya, India). *Remote Sens. Environ.* **108**, 327–338.
- Fujita, K. & Ageta, Y. 2000 Effects of summer accumulation on glacier mass balance on the Tibetan Plateau revealed by mass balance model. *J. Glaciol.* **46** (153), 244–252.

- Gardelin, M., Bergström, S., Carlsson, B., Graham, L. P. & Lindström, G. 2003 *Climate change and water resources in Sweden-analysis of uncertainties*. *Adv. Global Change Res.* **10**, 189–207.
- Hagg, W., Braun, L. N., Kuhn, M. & Nesgaard, T. I. 2007 *Modeling of hydrological response to climate changing glacierized Central Asian catchments*. *J. Hydrol.* **332** (1–2), 40–53.
- Hock, R. 2003 *Temperature index melt modeling in mountain areas*. *J. Hydrol.* **282** (1–4), 104–115.
- Hottelet, C., Braun, L. N., Leibundgut, C. & Rieg, A. 1993 *Simulation of snowpack and discharge in an alpine karst basin*. *Snow Glacier Hydrol.* **218**, 249–260.
- Hou, Q. & Wulan, B. T. E. 2006 *Analysis of climate change and its effect on soil moisture over Inner Mongolia typical steppe in recent 40 years*. *Meteorol. Sci. Technol.* **34** (1), 102–106.
- Jansson, P., Hock, R. & Schneider, P. 2003 *The concept of glacier storage: a review*. *J. Hydrol.* **282**, 116–129.
- Jost, G., Moore, R. D., Menounos, B. & Wheate, R. 2012 *Quantifying the contribution of glacier runoff to streamflow in the upper Columbia River Basin, Canada*. *Hydrol. Earth Syst. Sci.* **16**, 849–860.
- Kang, E. S., Cheng, G. D., Lan, Y. C. & Jin, H. J. 1999 *A model for simulating the response of runoff from the mountainous watersheds of inland river basins in the arid area of northwestern China to climate changes*. *Sci. China (Series D)* **42** (S1), 52–63.
- Kang, E. S., Cheng, G. D., Lan, Y. C. & Zhang, J. S. 2002 *Application of a conceptual hydrological model in the runoff forecast of a mountainous watershed*. *Adv. Earth Sci.* **17** (1), 18–26.
- Kavetski, D. & Clark, M. P. 2010 *Ancient numerical daemons of conceptual hydrological modeling: 2. Impact of time stepping schemes on model analysis and prediction*. *Water Resour. Res.* **46** (10), 1–27.
- Kazuo, A. 1995 *Two Himalaya Range high uplift since the 17ma*. *J. Geosci Transl.* **10** (2), 14–19.
- Konz, M. & Seibert, J. 2010 *On the value of glacier mass balances for hydrological model calibration*. *J. Hydrol.* **385**, 238–246.
- Kulkarni, A. V., Randhawa, S., Rathore, B. P., Bahuguna, I. M. & Sood, R. K. 2002 *Snow and glacier melt runoff model to estimate hydropower potential*. *J. Indian Soc. Remote Sens.* **30** (4), 220–228.
- Li, L. & Xu, C. Y. 2014 *The comparison of sensitivity analysis of hydrological uncertainty estimates by GLUE and Bayesian method under the impact of precipitation errors*. *Stoch. Environ. Res. Risk Assess.* **28** (3), 491–504.
- Li, L., Ngongondo, C. S. & Xu, C. Y. 2013 *Comparison of the global TRMM and WFD precipitation datasets in driving a large-scale hydrological model in Southern Africa*. *Hydrol. Res.* **44** (5), 770–788.
- Liden, R. & Harlin, J. 2000 *Analysis of conceptual rainfall-runoff modeling performance indifferent climates*. *J. Hydrol.* **238** (3–4), 231–247.
- McIntyre, N., Ballard, B. & Bruen, M. 2013 *Modeling the hydrological impacts of rural land use change*. *Hydrol. Res.* **45** (6), 737–754.
- Menzeil, L. & Burger, G. 2002 *Climate changes scenarios and runoff response in the Mulde catchment (Southern Elbe, Germany)*. *J. Hydrol.* **267**, 53–64.
- Moore, R. D., Fleming, S. W., Menounos, M., Wheate, R., Fountain, A., Stahl, K., Holm, K. & Jakob, M. 2009 *Glacier change in Western North America: influences on hydrology, geomorphic hazards and water quality*. *Hydrol. Process.* **23**, 42–61.
- Nash, J. & Sutcliffe, J. V. 1970 *River flow forecasting through conceptual models part I – a discussion of principles*. *J. Hydrol.* **10**, 282–290.
- Nourali, M., Ghahraman, B. & Pourrezabilondi, M. 2016 *Effect of formal and informal likelihood functions on uncertainty assessment in a single event rainfall-runoff model*. *J. Hydrol.* **540**, 549–564.
- Pu, J. C., Su, Z., Yao, T. D. & Xie, Z. C. 1998 *Mass balance on Xiao Dongkemadi Glacier and Hailuoguo Glacier*. *J. Glaciol. Geocryol.* **20** (4), 408–412.
- Seibert, J. 2005 *HBV Light (Version 2) User's Manual*. Environmental Assessment Department, Uppsala University, Sweden, pp. 1–32.
- Seibert, J. & Vis, M. J. P. 2012 *Teaching hydrological modeling with a user-friendly catchment-runoff-model software package*. *Hydrol. Earth Syst. Sci.* **16**, 3315–3325.
- Sun, Y. H., Huang, X. D., Wang, W., Feng, Q. S., Li, H. X. & Ling, T. G. 2014 *Spatio-temporal changes of snow cover and snow water equivalent in the Tibetan Plateau during 2003–2010*. *J. Glaciol. Geocryol.* **36** (6), 1337–1344.
- Sun, M. P., Yao, X. J., Li, Z. Q. & Zhang, M. J. 2015 *Hydrological processes of glacier and snow melting and runoff in the Urumqi River source region, eastern Tianshan Mountains, China*. *J. Geog. Sci.* **25** (2), 149–164.
- Wang, X. Y., Tao, Y., Xu, C. Y., Yong, B. & Shi, P. F. 2019 *Understanding the discharge regime of a glacierized alpine catchment in the Tianshan Mountains using an improved HBV-D hydrological model*. *Glob. Planet. Change* **172**, 211–222.
- Yin, Z., Mu, Z., Gao, R., Zhou, Y. & Tang, R. 2017 *Application of HBV hydrological model considering glacier melt in Western Tianshan*. *J. Hydroel. Eng.* **11**, 42–49.
- Zhang, Y. & Yao, T. 2002 *Hydrological Processes and Their Features*. Geological Press, Beijing, pp. 199–206.
- Zhang, Y., Yao, T., Pu, J., Xiao, C. & Kang, S. 1997 *The features of hydrological processes in the Dongkemadi River Basin, Tanggula Pass, and Tibetan Plateau*. *J. Glaciol. Geocryol.* **19** (3), 214–222.
- Zhao, Q. D., Ye, B. S., Ding, Y. J., Zhang, S. Q., Yi, S. H., Wang, J., Shangguan, D. H., Zhao, C. & Han, H. D. 2013 *Coupling a glacier melt model to the Variable Infiltration Capacity (VIC) model for hydrological modeling in north-western China*. *Environ. Earth Sci.* **68** (1), 87–101.

Zhao, C., Zhang, L. H., Li, J. L., Tian, J., Wu, W. Z., Jin, X. & Zhang, X. F. 2014 Analysis of the relationships between the spatial variations of soil moisture and the environmental factors in the upstream of the Heihe River watershed. *J. Lanzhou Univ. (Nat. Sci.)* **3**, 338–347.

Zhu, G. F., He, Y. Q., Qin, D. H., Gao, H. K., Pu, T., Chen, D. D. & Wang, K. 2016 The impacts of climate change on hydrology in a typical glacier region-A case study in Hailuo Creek watershed of Mt. Gongga in China. *Sci. Cold Arid Reg.* **8** (3), 227–240.

First received 30 January 2020; accepted in revised form 4 August 2020. Available online 21 October 2020